Available online at www.sciencedirect.com
ScienceDirect
Journal of Power Sources 167 (2007) 200–205
JOURNAL OF POWER SOURCES
www.elsevier.com/locate/jpowsour

Short communication

A simple, cheap soft synthesis routine for $LiFePO_4$ using iron(III) raw material

L.N. Wang [a], Z.G. Zhang [a], K.L. Zhang [a,b,*]

[a] *College of Chemistry and Molecular sciences, Wuhan University, Wuhan 430072, China*
[b] *Centre of Nanoscience and Nanotechnology Research, Wuhan University, Wuhan 430072, China*

Received 28 October 2006; received in revised form 1 December 2006; accepted 1 February 2007
Available online 11 February 2007

Abstract

An order olivine structure $LiFePO_4$ was synthesized with a simple rheological phase reaction (RPR) of $LiOH{\cdot}H_2O$ and $FePO_4{\cdot}4H_2O$ in the presence of PEG as a reductive agent and carbon source. A required amount of water was added to the starting materials to form the rheological precursor and decomposed at 700 °C to form the crystalline phase $LiFePO_4$ directly, without ball-milling, preparation of intermediates, pre-sintering and post-deposition treatment. Fine particles with an average particle size about 216 nm are examined by scanning electron microscopy (SEM) and optical particle size analyzer. An initial discharge capacity of 157 mAh g^{-1} was achieved for the as-prepared $LiFePO_4$ material with a rate of 0.1*C* (17 mA g^{-1}), what's more, this material shows excellent specific capacity, charge–discharge efficiency and cycle efficiency at high current rates, almost no capacity loss can be observed up to 40 cycles with the rate of 1, 2 and 3*C* at room temperature. The simple, cheap process as well as the excellent high-rate performance makes this RPR method feasible commercially.

Keywords: $LiFePO_4$; Rheological phase reaction; $FePO_4{\cdot}4H_2O$; High-rate performance

1. Introduction

Due to its overwhelming advantages of low toxicity, good thermal stability and relatively high theoretical capacity, olivine type $LiFePO_4$, which was first introduced as a lithium battery cathode material by Padhi et al. appears as a potential candidate to be used as positive electrode in next generation of Li-ion batteries [1–5]. As a material, however, $LiFePO_4$ is an insulator, which seriously limits its rate capability in lithium cells. It shows high electrochemical properties only at low charge/discharge rates owing to its low electronic conductivity and low lithium ion motion ability [6,7]. Therefore, research on this insulating compound was up to now mostly devoted to enhance the composite's conductivity by metal doping [8,9] or coating with the electronically conductive materials like carbon, metal and metal oxide [10–12].

Other possible means of improving the rate performance of $LiFePO_4$ materials are those of enhancing its ionic/electronic conductivity by optimization of particles with suitable preparation procedures. In addition to the traditional solid-state reaction synthesis routine, alternative synthesis processes including sol–gel, hydrothermal, co-precipitation, microwave heating, etc. have developed continually [11,13–15]. However, many obstacles have been encountered for some synthesis methods reported from a laboratory process to mass production because of the complicated synthesis techniques, the hard-controlled synthesis situation and the relatively high cost Fe(II) precursor, which was used in most cases. What is more, additional care is required to prevent oxidization of the resulting precursors because Fe (II) ions are much easier to oxidize in air, which makes the above synthesis processes less effective. In current time, it is urgent to develop a simple, cheap and efficient method for the mass production of $LiFePO_4$ cathode material.

Recently, Prosini et al. [16] synthesized $LiFePO_4$ by chemical lithiation of $FePO_4$ by LiI, Wang et al. [17] synthesized $LiFePO_4$-C from amorphous $FePO_4{\cdot}4H_2O$ through a solid–liquid phase reaction using $(NH_4)_2SO_3$ as the reducing agent and Ying et al. [18] synthesized $Li_{0.97}Cr_{0.01}FePO_4$-C with $Fe(NO_3)_3$ as iron source via a controlled crystallization–carbothermal reduction method using sucrose

* Corresponding author. Tel.: +86 27 87218484; fax: +86 27 68754067.
E-mail address: klzhang@whu.edu.cn (K.L. Zhang).

0378-7753/$ – see front matter © 2007 Elsevier B.V. All rights reserved.
doi:10.1016/j.jpowsour.2007.02.002

as a reductive agent and carbon source, all of which showed good electrochemical performance. However, the above synthesis techniques are complicated and hard-controlled somewhat for the amorphous intermediates $FePO_4{\cdot}xH_2O$ or NH_4FePO_4 should be prepared first and the impurity ions such as I^- or SO_4^{2-} was introduced. Barker et al. [19] and Kim et al. [20] synthesized $LiFePO_4$-C based on a carbothermal reduction (CTR) reaction using Fe_2O_3 as the starting material, however, the resources of [Fe] and [PO_4] in $LiFePO_4$ come from two compounds, which are hard to mix at the atomic level.

Previously, the rheological phase reaction (RPR) has been reported by our group as an efficient soft chemistry method to prepare electrodes or other materials [21–24]. In this study, $LiFePO_4$-C cathode material with nano-sized fine particles was synthesized from inexpensive $FePO_4{\cdot}4H_2O$ raw material by employing polyethylene glycol (PEG) as a novel reducing agent and carbon source with this simple, cheap soft chemistry method—RPR. The precursor of $LiFePO_4$-C is very easy to make in a short time, and then the resulting precursor is heated in inert atmosphere to get the powders of $LiFePO_4$-C directly via this PRR method. No need of ball-milling, preparation of intermediates, pre-sintering and post-deposition treatment compared with traditional solid-state reaction synthesis routine and some other complicated synthesis techniques. The microstructure and the electrochemical properties of the as-prepared $LiFePO_4$-C were investigated carefully.

2. Experimental

Stoichiometric amounts of $LiOH{\cdot}H_2O$, $FePO_4{\cdot}4H_2O$ and polyethylene glycol (PEG; mean molecular weight of 10,000, 250 g PEG/mol $FePO_4$) powders were used as the starting materials by RPR method. As shown in the flow chart (Fig. 1), they were mixed by grinding for 10 min, and then appropriate amount of de-ionized water was added to get a rheological body. Finally, the resulting precursor was heated in a tube furnace to get the powders of $LiFePO_4$-C at 700 °C for 12 h in Ar flow.

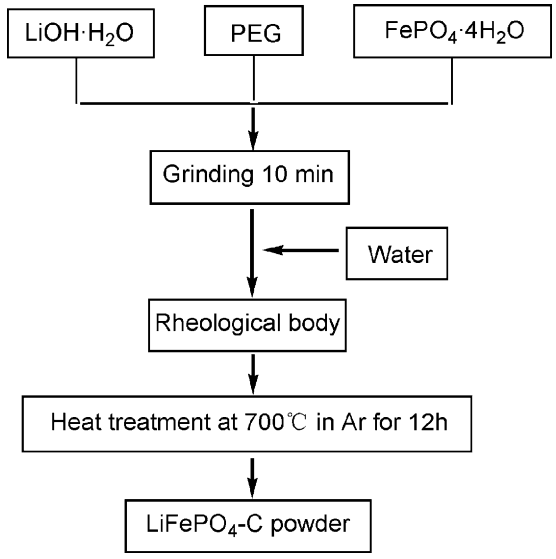

Fig. 1. Flow chart of the RPR synthesis process.

X-ray diffraction (XRD) profile of the sample was carried out on a shimadzu XRD-6000 diffractometer using Cu $K\alpha_1$ radiation. The morphology and microstructure was observed using scanning electron microscopy (SEM) with Hitachi FEG SEM and high-resolution transmission electron microscope (HRTEM) with JEOL JEM 2010 FEF. The particles size distribution was determined by the optical particle size analyzer (Mastersizer 2000, England). The amount of carbon was determined by element analyzer (FLASH 112SERIES, Italy). The surface elements' content of $LiFePO_4$-C powders was determined by an X-ray photoelectron spectrometer (XPS, Kratos Model XSAM800) equipped with an Mg Kα achromatic X-ray source (1235.6 eV).

For the cell measurement, the cathode performance was examined by a Shenzhen Neware battery program-controlled test system. The $LiFePO_4$-C material was mixed with 20 wt.% carbon black and 5 wt.% PTFE. The mixture was pressed onto nickel grid as the cathode, pure lithium as the anode, 1 M $LiClO_4$ (EC:DMC = 1:1) as the electrolyte, a Celguard 2400 (American) micro-porous membrane for the separator. The cells were charge–discharged between 2.0 and 4.4 V at room temperature. Note that the charge and discharge rates were equal under a given current density and specific capacities were calculated based on the mass of $LiFePO_4$-C composites.

3. Results and discussion

In this work, $LiFePO_4$ was synthesized under the assumption that the following reaction occurred:

$$2n\mathrm{LiOH{\cdot}H_2O} + 2n\mathrm{FePO_4{\cdot}4H_2O} + \mathrm{HO(C_2H_4O)}_n\mathrm{H} \rightarrow 2n\mathrm{LiFePO_4} + 2n\mathrm{C} + (13n+1)\mathrm{H_2O}$$

During the heating of the PEG-contained precursor, Fe^{3+} was reduced to Fe^{2+} with the help of hydrogen and carbon as the reducing agent, which are generated from the decomposition of PEG, producing a strong reductive atmosphere.

The X-ray diffraction pattern of the as-prepared $LiFePO_4$-C composite is shown in Fig. 2. All peaks can be indexed as pure and well-crystallized $LiFePO_4$ phase with an ordered olivine structure and a space group of Pnma (JCPDS card no. 83–2092). Previously, there was report that some detectable impurities such as Li_3PO_4 has been identified in $LiFePO_4$ prepared by conventional solid-state reaction using the Fe(II) raw material. In contrast, we did not detect any impurities, indicating that this RPR routine using the Fe(Ⅲ) raw material is a feasible method to prepare pure $LiFePO_4$. No evidence of diffraction peaks for crystalline carbon (graphite) appeared in the diffraction pattern, which indicates that the carbon generated from PEG is amorphous carbon and its presence does not influence the structure of $LiFePO_4$. Basing on Scherrer's equation $d = 0.9\lambda/\beta_{1/2}\cos\theta$, one can know that with the increasing of the dimension of crystal grains (d), the full-width-at-half-maximum (FWHM) length of the diffraction peak ($\beta_{1/2}$) is decreasing on a 2θ scale. It is found the $\beta_{1/2}$ (Fig. 2) is a little wide, which indicate that the crystal grains are small. The calculated crystal grain size is about 23 nm from the Scherrer's equation according to D_{111}, D_{121} and D_{131}

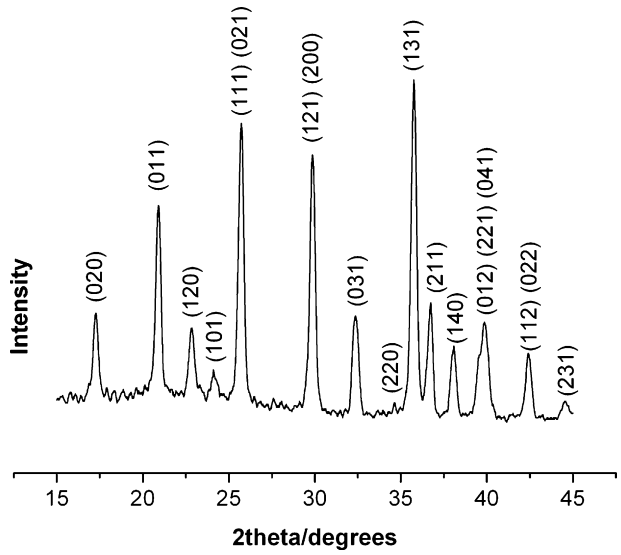

Fig. 2. XRD pattern of as-prepared $LiFePO_4$-C composite.

values. The result indicates the soft RPR process and the carbon reduced from the decomposition of PEG during the heating prohibited the growth of $LiFePO_4$ grains efficiently. The amount of carbon in the $LiFePO_4$-C composite is about 6.13 wt.% through the element analysis (EA), in other words, the molar ratio of C:$LiFePO_4$ is about 0.86. In order to examine the surface elements' content of the $LiFePO_4$-C powders, XPS analysis was performed, as shown in Fig. 3, a sharp peak at about 285.3 eV corresponding to C 1s with a high intensity is seen. The Binding Energy of Fe 2p, O 1s and P 2p are determined to be 711.4, 532.5 and 133.9 eV respectively. However, as Lee et al. reported [25], Li 1s emission peak is not seen clearly because it is superposed on the Fe 3p peak at about 56 eV, precluded accurate determination of its binding energy and estimation of the element content. According to XPS analysis, on the surface of $LiFePO_4$-C powders, the C:P molar ration thus obtained is about 19:1, which indicates the surface composition should be mainly the carbon and carbon is coated on the $LiFePO_4$ particles rather perfectly [18]. Moreover, the result of XPS analysis shows that the as-prepared material comprised of all the constituent elements of $LiFePO_4$.

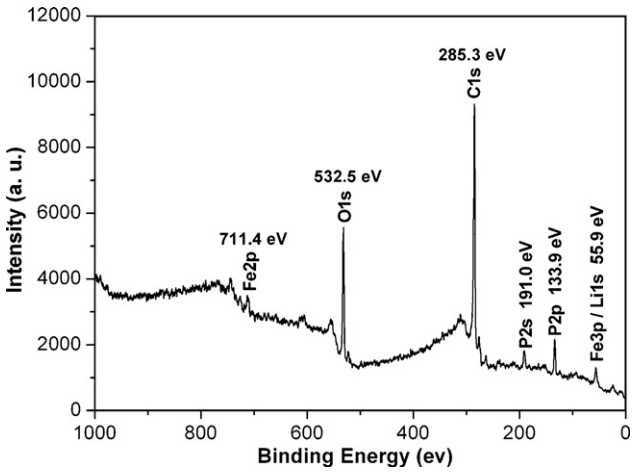

Fig. 3. XPS spectra of as-prepared $LiFePO_4$-C powders.

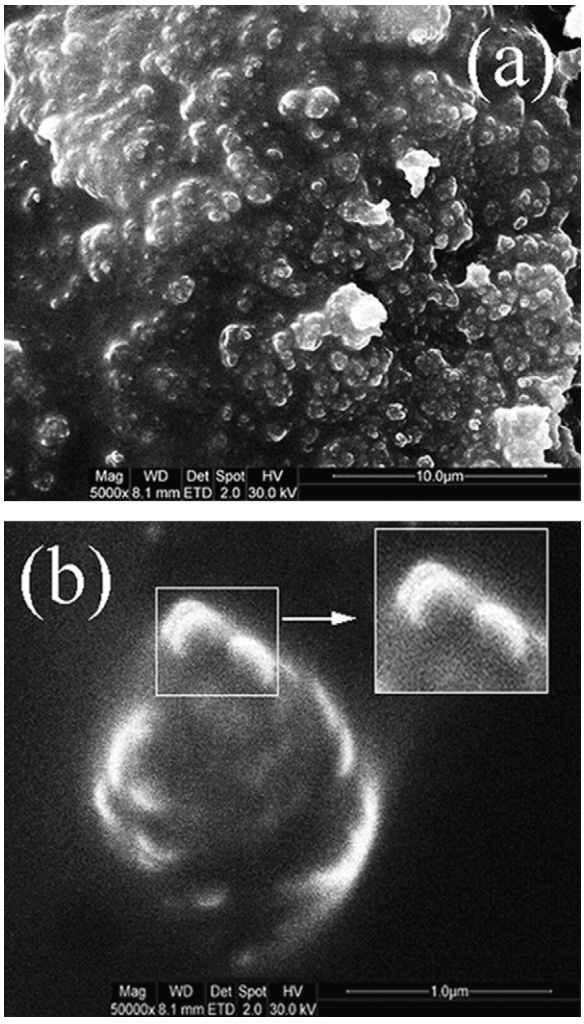

Fig. 4. SEM images of as-prepared sample. (a) Overall morphology for $LiFePO_4$-C; (b) one particle in the image (a). Inset: magnification of the selected area.

The morphology for $LiFePO_4$-C powders was observed on SEM, as shown in Fig. 4. We can see that lots of independent particles pack closely between the porous structure of carbon and the average particle size is around 0.8 μm (Fig. 4a). The image of one particle selected randomly from Fig. 4a is shown in Fig. 4b, which can be seen clearly that the particle is a kind of secondary particle composed of small size particles (around 200 nm). To further understand this investigation, we ran particles size distribution analysis on the sample, as shown in Fig. 5. The value at 50% cumulative population ($d_{50\%}$) represents the average particle size. The average particle size was 216 nm for the as-prepared $LiFePO_4$-C powder. The result is consistent with the result of SEM morphology. However, the particle distribution has two regions, the peak around smaller particle size should be due to $LiFePO_4$-C powders, and the other peak at lager particle size region can ascribe to agglomerated large particles that were not dispersed perfectly. Note that the average particle size of the synthesized $LiFePO_4$ is larger than its crystal grain size that calculated from XRD patterns, implying that the particles

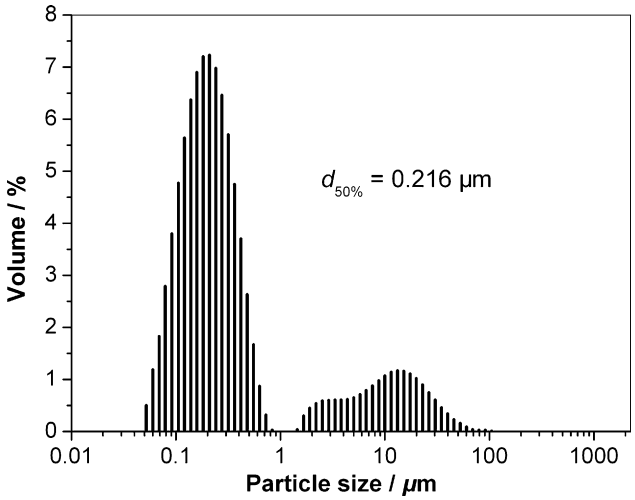

Fig. 5. Particle size distribution of as-prepared $LiFePO_4$-C sample.

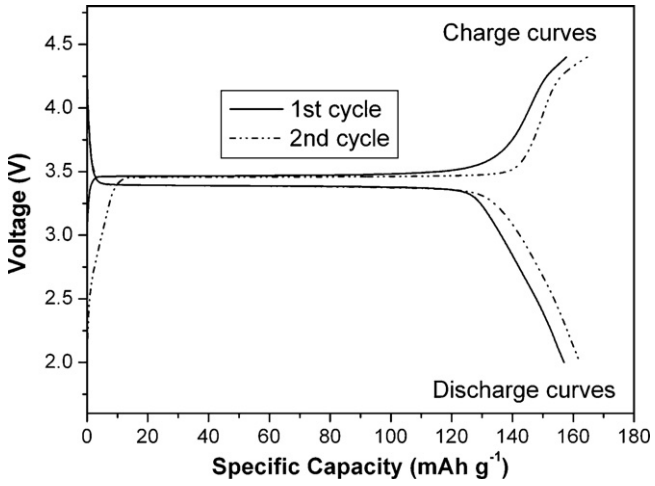

Fig. 7. Typical charge/discharge curves of the Li/$LiFePO_4$-C cell at low current density (0.1*C*).

are formed from the agglomeration of several grains [26], which is confirmed by the TEM images, as shown in Fig. 6. From the TEM images, it can be seen clearly that uniform fine $LiFePO_4$ crystal grains (<50 nm) disperse in the carbon webs, most of the grains are wrapped and connected with carbon. The observation of SEM and TEM images accords with the results of XRD and XPS analysis.

Based on the above analysis, the formation of the $LiFePO_4$-C powders during the heating process was proposed as follows. First, a large number of very small nanometer $LiFePO_4$ crystal grains grow in the carbon network, then the grains aggregate together and form the nanometer $LiFePO_4$ particles, and finally, the secondary $LiFePO_4$ particles are formed by the agglomeration of several nanometer $LiFePO_4$ particles, which was closely connected by the carbon. The conductivity of $LiFePO_4$-C compound would be enhanced due to existence of the formed carbon between the crystal grains, the $LiFePO_4$ particles and the close connection of the secondary particles by the carbon network.

Typical charge/discharge curves of the Li/$LiFePO_4$-C cell in the first two cycles with low current density (0.1*C*) are plotted in Fig. 7. The first discharge capacity is 157 mAh g^{-1} and then increase to 162 mAh g^{-1} in the second cycle, which maybe caused by the "activation" of the first cycle reaction [17]. A flat and long voltage curve around 3.4 V indicates that

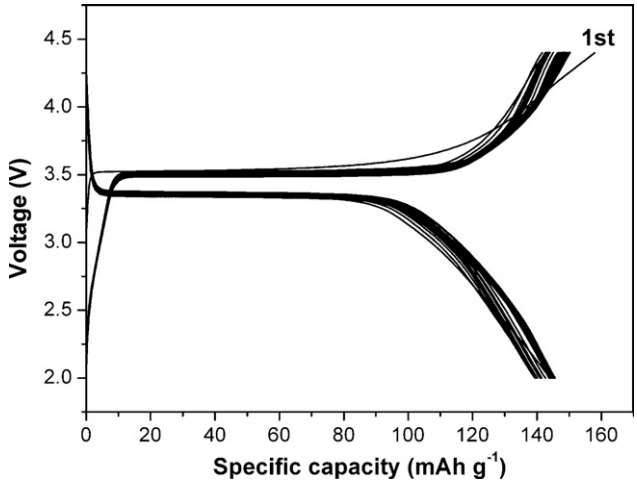

Fig. 8. Typical charge/discharge curves of the Li/$LiFePO_4$-C cell in the first 40 cycles at high current density (1*C*).

the two-phase redox reaction proceeds via a first-order transition between $LiFePO_4$ and $FePO_4$. Fig. 8 shows the typical charge/discharge curves of the Li/$LiFePO_4$-C cell in the first 40 cycles at high current density (1*C*), the first cycle discharge capacity is 144 mAh g^{-1}. One can see that the polarization of the

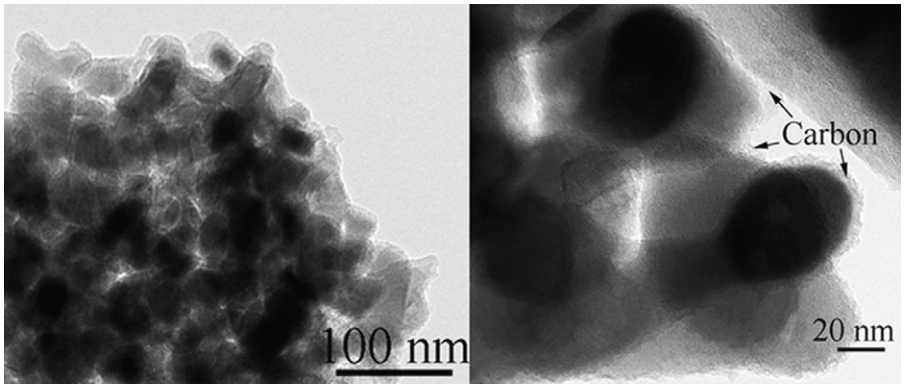

Fig. 6. TEM images of as-prepared $LiFePO_4$-C sample.

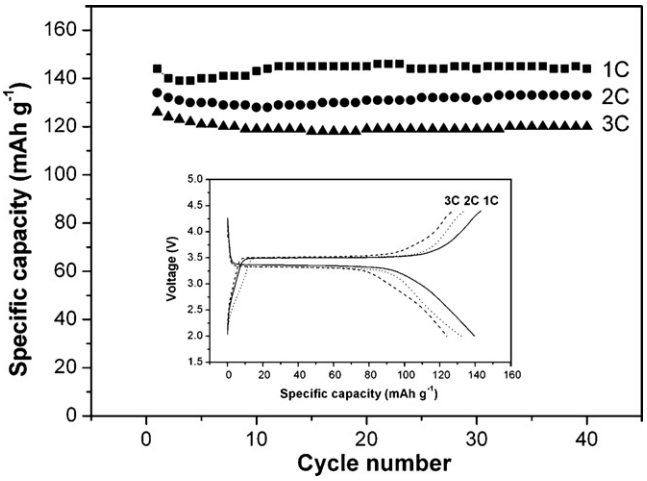

Fig. 9. The cycle performance of $LiFePO_4$-C composite electrode. Inset means the charge/discharge curves of $LiFePO_4$-C in the second cycle.

following cycles decreased and the charge/discharge efficiency increased compared with the first cycle. The charge/discharge efficiency is above 96% (except the initial cycle) and the cycle efficiency is near to 100% up to 40 cycles. It is still remained good stability and reversibility (no obvious polarization and very flat 3.4 V plateau can be seen) even after 40 cycles. However, the initial capacity loss increased and the capacity of the following cycle is not increased obviously compared with the cells cycled with low rate (Fig. 7), which maybe caused by the difficulty in utilizing large particles because of the diffusion limit of the lithium through the $LiFePO_4/FePO_4$ interface at high current density. Fig. 9 shows the specific capacity of the $LiFePO_4$-C composite in function of the cycle number with different charge/discharge rates at room temperature. The initial discharge capacities were 144, 134 and 126 mAh g^{-1} at the 1, 2 and 3*C* rate, respectively. The capacities were stably retained up to 40 cycles. Note that at a given *C*-rate, the charge and discharge current density are equal to ensure fast charging/discharging, which is different from some reports that to charge the cell with very low current density to get high capacity and then to discharge with high current density when examine the high-rate performance of $LiFePO_4$ materials, thus a comparative long time would be consumed and it is not convenient for the use of electric vehicles and other mobile devices. Moreover, the capacity is based on the $LiFePO_4$-C composite instead of considering the $LiFePO_4$ active material merely. Inset was the charge-discharge curves of the Li/$LiFePO_4$-C cells in the second cycle, a flat voltage plateau can be observed even at the rate as high as 3*C*. And the electrochemical reactions in Li-ion cells were also can be confirmed by cyclic voltammograms (CV) of $LiFePO_4$-C electrodes. The reduction and oxidation peaks, corresponding to the two-phase charge/discharge reaction of Fe^{2+}/Fe^{3+} redox couple, is still obvious even at a scan rate of 2 mV s^{-1}, which corresponds to about 7*C* cycling rate. The electrochemical performance of the $LiFePO_4$-C composite made from this RPR route is similar or improved compared with the published data about the $LiFePO_4$ materials made from Fe(III) raw materials in the recent studies [16–20,27]. The high-rate performance indicates that the synthesized $LiFePO_4$-C composite would be well suited for cathode materials of high-power lithium batteries and the RPR using iron(III) as raw material is a very charming potential method for mass production, because it improves the cell performance of the $LiFePO_4$ at the same time decreases the cost of the preparation through very simple process.

4. Conclusions

$LiFePO_4$-C composite is successfully synthesized by a simple RPR method using Fe(III) as the raw material with PEG as the carbon source and reductive agent. The cell performance was improved because the conductivity was well improved by the closely packed particles through the connection of carbon webs. An initial capacity of 157 mAh g^{-1} was obtained at 0.1*C* and excellent high-rate performance was also achieved, no obvious capacity loss and polarization can be observed at high current density up to 40 cycles. The process is also very cheap, efficient and reproducible, moreover, since no noxious gas was released during the heating treatment, the process is more environmental friendly and feasible commercially than other methods.

Acknowledgements

This work was supported by the National Natural Science Foundation of China (No. 20071026). The authors are grateful to the Centre of Nanoscience and Nanotechnology Research of Wuhan University for their experimental assistance.

References

[1] A.K. Padhi, K.S. Nanjundaswamy, J.B. Goodenough, J. Electrochem. Soc. 144 (1997) 1188.
[2] A.K. Padhi, K.S. Nanjundaswamy, C. Masquelier, S. Okada, J.B. Goodenough, J. Electrochem. Soc. 144 (1997) 1609.
[3] A.S. Andersson, J.O. Thomas, J. Power Sources 97–98 (2001) 498.
[4] N. Ravet, Y. Chouinard, J.F. Magnan, S. Besner, M. Gauthier, M. Armand, J. Power Sources 97–98 (2001) 503.
[5] A. Yamada, S.-C. Chung, K. Hinokuma, J. Electrochem. Soc. 148 (2001) A224.
[6] A.S. Andersson, J.O. Thomas, B. Kalska, L. Haggstrom, Electrochem. Solid State Lett. 3 (2000) 66.
[7] T.-H. Cho, H.-T. Chung, J. Power Sources 133 (2004) 272.
[8] G.X. Wang, S.L. Bewlay, K. Konstantinov, H.K. Liu, S.X. Dou, J.-H. Ahn, Electrochim. Acta 50 (2004) 443.
[9] S.-Y. Chung, J.T. Bloking, Y.-M. Chiang, Nat. Mater. 1 (2002) 123.
[10] H. Huang, S.-C. Yin, L.F. Nazar, Electrochem. Solid State Lett. 4 (2001) A170.
[11] F. Croce, A.D. Epifanio, J. Hassoun, A. Deptula, T. Olczac, B. Scrosati, Electrochem. Solid State Lett. 5 (2002) A47.
[12] H. Huang, S.-C. Yin, L.F. Nazar, J. Electrochem. Soc. 149 (2002) 1184.
[13] S. Franger, F.L. Cras, C. Bourbon, H. Rouault, J. Power Sources 119–121 (2003) 252.
[14] K.S. Park, J.T. Son, H.T. Chung, S.J. Kim, C.H. Lee, H.G. Kim, Electrochem. Commun. 5 (2003) 839.
[15] S.F. Yang, P.Y. Zavalij, M.S. Whittingham, Electrochem. Commun. 3 (2001) 505.
[16] P.P. Prosini, M. Carewska, S. Scaccia, P. Wisniewski, S. Passerini, M. Pasquali, J. Electrochem. Soc. 149 (2002) A886.
[17] Y.Q. Wang, J.L. Wang, J. Yang, Y.N. Nuli, Adv. Funct. Mater. 16 (2006) 2135.

[18] J.R. Ying, M. Lei, C.Y. Jiang, C.R. Wan, X.M. He, J.J. Li, L. Wang, J.G. Ren, J. Power Sources 158 (2006) 543.
[19] J. Barker, M.Y. Saidi, J.L. Swoyer, Electrochem. Solid State Lett. 6 (2003) A53.
[20] C.W. Kim, M.H. Lee, W.T. Jeong, K.S. Lee, J. Power Sources 146 (2005) 534.
[21] H. Tang, C.Q. Feng, Q. Fan, T.M. Lei, J.T. Sun, L.J. Yuan, K.L. Zhang, Chem. Lett. 8 (2002) 822.
[22] C.C. Ai, M.C. Yin, C.W. Wang, J.T. Sun, J. Mater. Sci. 39 (2004) 1077.
[23] C.Q. Feng, H. Tang, K.L. Zhang, J.T. Sun, Mater. Chem. Phys. 80 (2003) 573.
[24] L.J. Yuan, M.C. Yin, E.T. Yuan, J.T. Sun, K.L. Zhang, Inorg. Chim. Acta 357 (2004) 89.
[25] J. Lee, A.S. Teja, J. Supercrit. Fluids 35 (2005) 83.
[26] K.-F. Hsu, S.-Y. Tsay, B.-J. Hwang, J. Power Sources 146 (2005) 529.
[27] M.-R. Yang, W.-H. Ke, S.-H. Wu, J. Power Sources 146 (2005) 539.